

Numerical Analysis of Damage Propagation for Discontinuous CFRTP

Keita GOTO, Shota OKUIZUMI

Masahiro ARAI, and Akinori YOSHIMURA

Department of Aerospace Engineering, Nagoya University (Japan)

Introduction

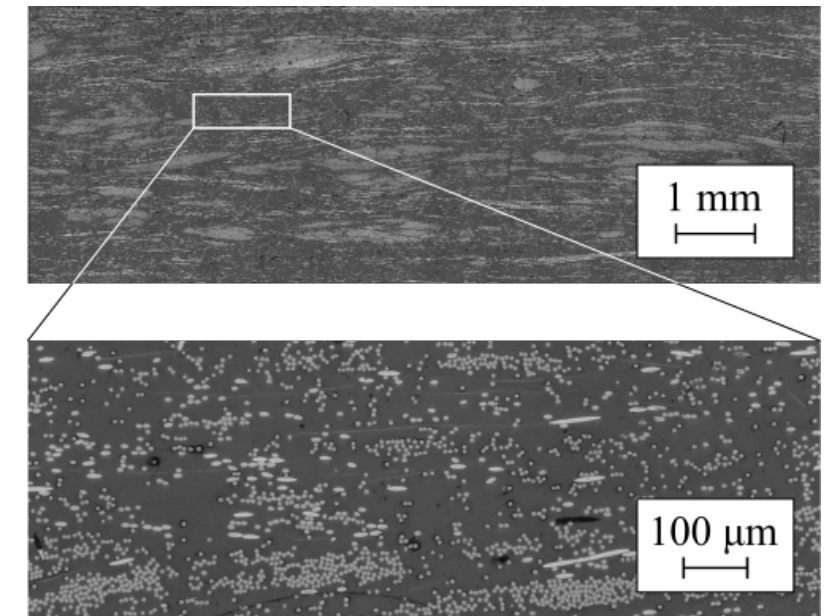
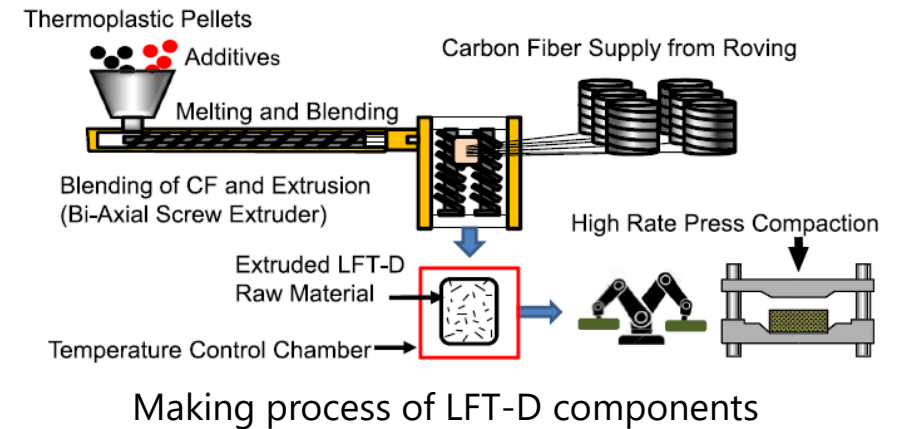
LFT-D (long fiber thermoplastic-direct)

- A type of discontinuous CFRTTP
- Long fiber length and high mechanical property
- Short cycle time in making process
- Expected to apply for automobile structures
- Complex internal structures owing to making process
- Difficult to predict (esp.) failure or fracture behavior

Objective

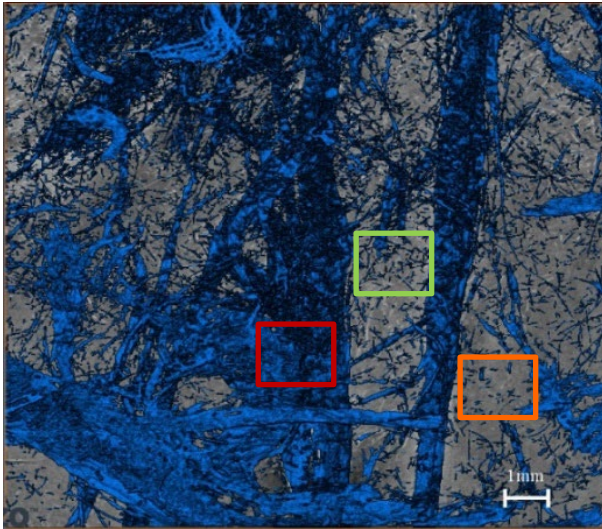
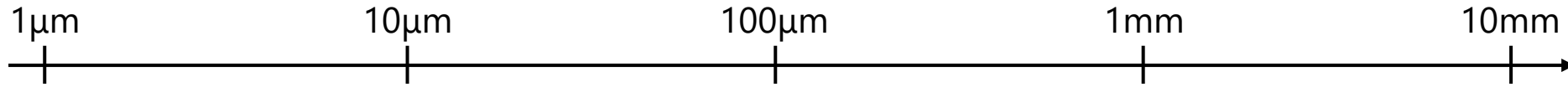
Mechanical property of LFT-D is evaluated based on multiscale numerical method.

- Internal structures of LFT-D are investigated.
- Characteristic structures are considered in FE models.
- Elasto-viscoplastic and damage propagation behavior of LFT-D are investigated by multiscale numerical method.

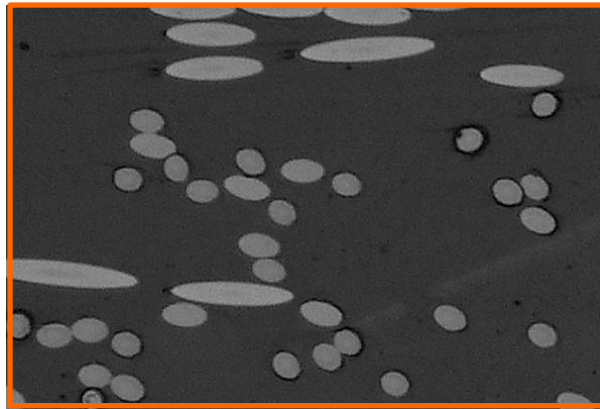


Cross-sectional images of LFT-D

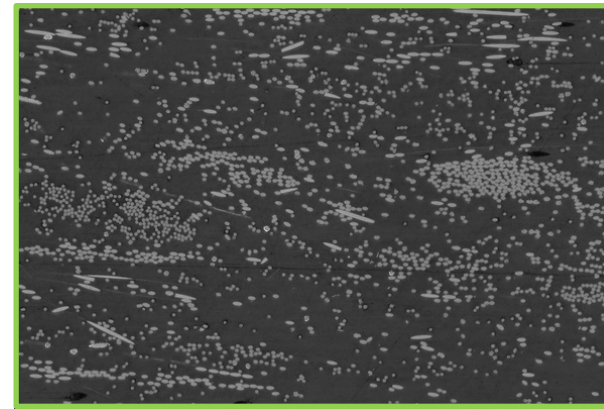
Multiscale internal structures of LFT-D



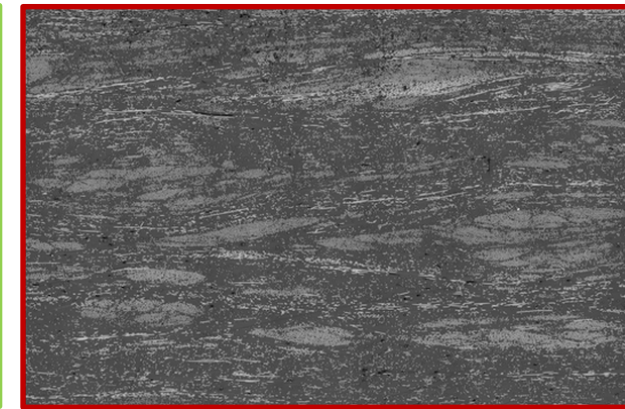
X-ray CT image of LFT-D
(Volume fraction = 20%)



Microscale
Dispersed carbon fibers
randomly distribute



Mesoscale
Short fiber bundles
randomly distribute

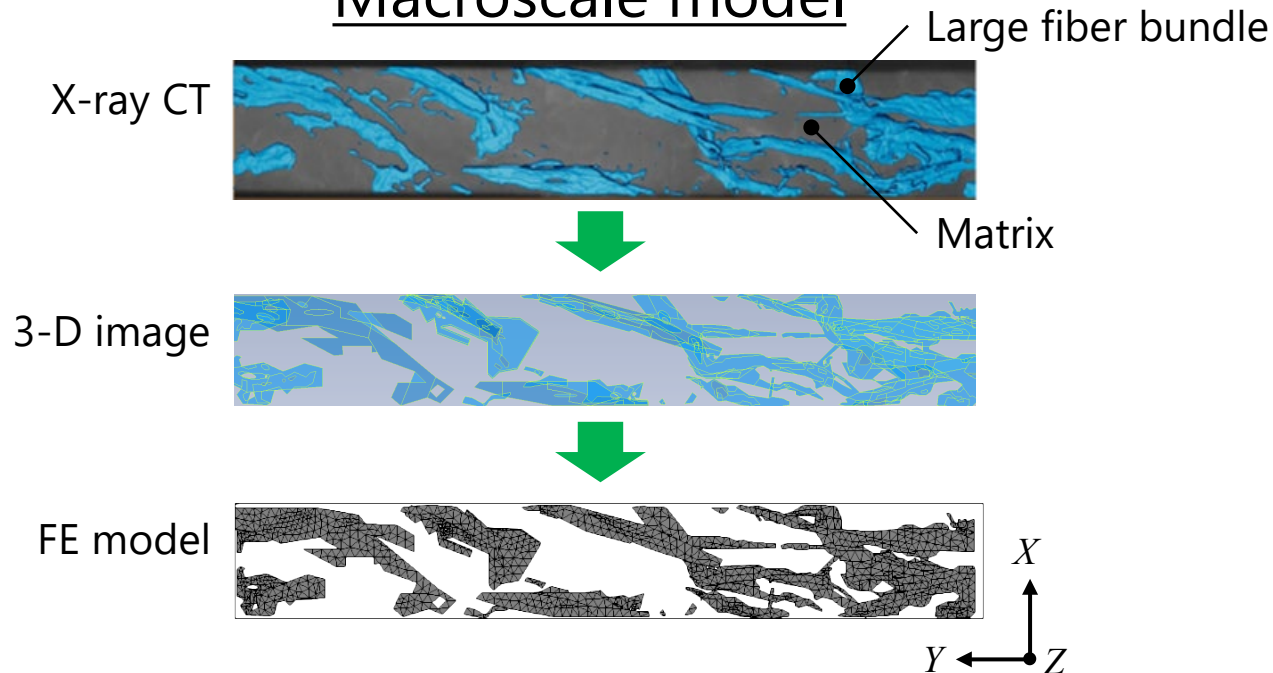


Macroscale
Large fiber bundles
characteristically distribute

- Characteristic and complex internal structures of LFT-D can be found from observation results.
- Internal structures of LFT-D are classified into three-scales (micro, meso, and macroscales).
- Finite element models considering characteristic structures in each scale are prepared.

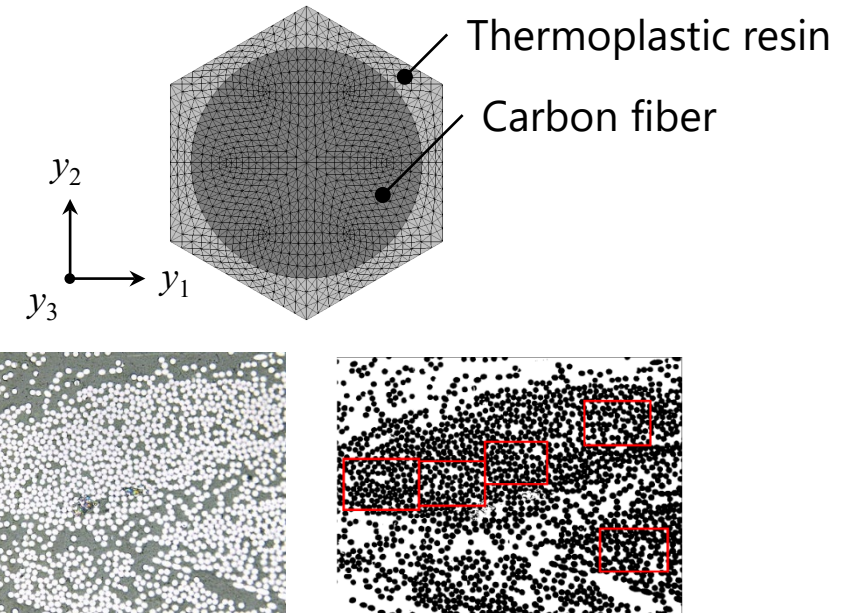
Finite element models

Macroscale model



- Made from CT image of tensile test specimen
- Discretization: 3-D tetrahedron elements
- Nodes: 12769, elements: 62628
- Fiber bundle volume fraction: 12%

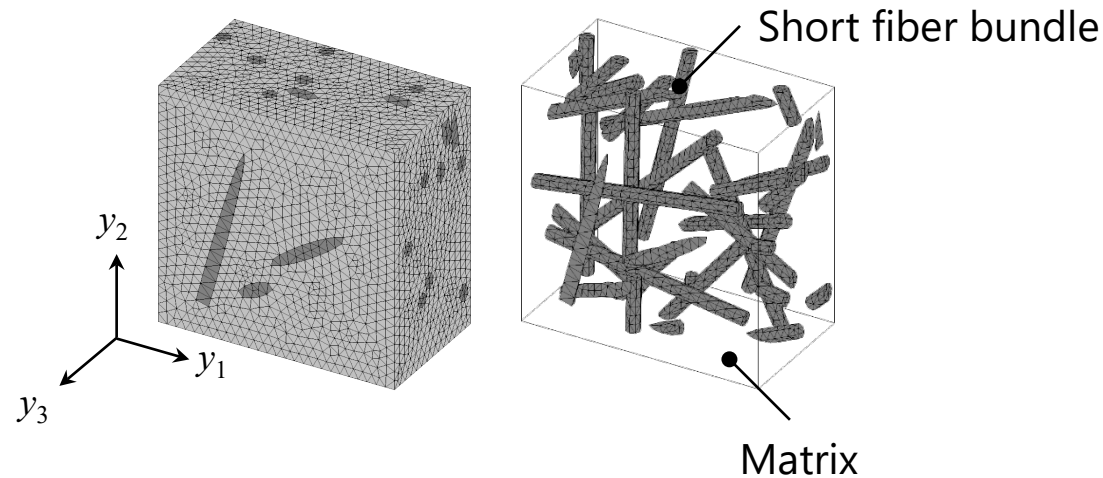
Fiber bundle internal model



- Made from binarization image of cross-sectional observation of fiber bundle
- Discretization: 2-D triangle elements
- Nodes: 757, elements: 1440
- Fiber volume fraction: 65%

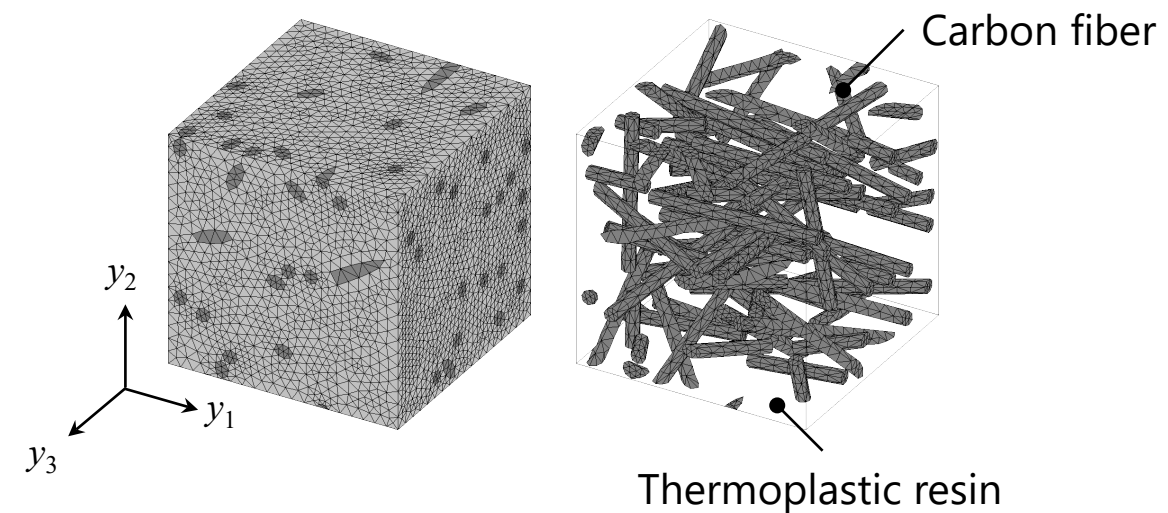
Finite element models

Mesoscale model



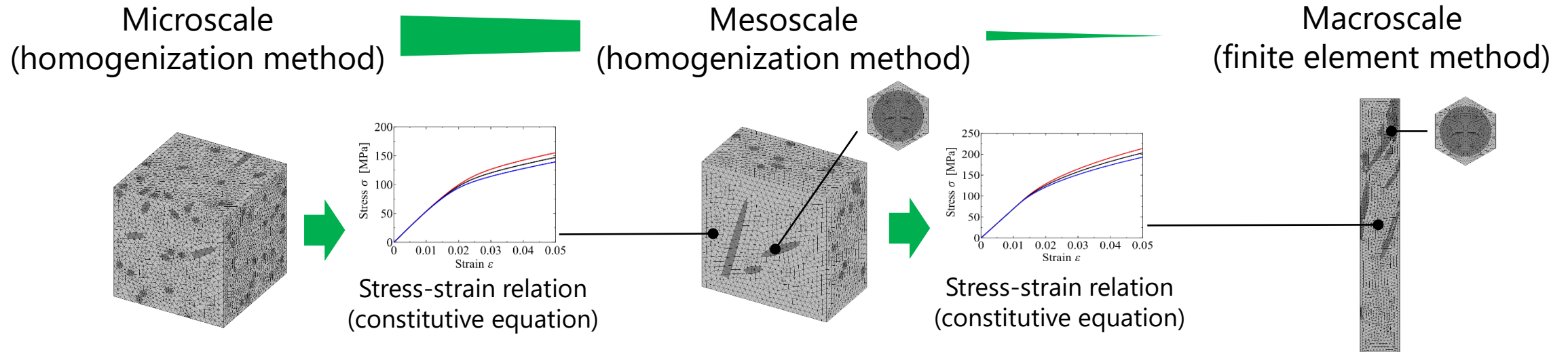
- Made from length/orientation distributions of short fiber bundles from image analyses
- Fiber bundles: 800μm-length, 48μm-diameter
- Discretization: 3-D tetrahedron elements
- Nodes: 17069, elements: 91415
- Fiber bundle volume fraction: 5.6%

Microscale model



- Assuming isotropic distribution of fibers
- Carbon fibers: 115μm-length, 7μm-diameter
- Discretization: 3-D tetrahedron elements
- Nodes: 14388, elements: 69087
- Fiber volume fraction: 9.6%

Multiscale numerical analysis procedure



1. In microscale, homogenization analyses are performed under several strain rate conditions. Obtained stress-strain curves are approximated by elasto-viscoplastic constitutive equations.
2. In mesoscale, homogenization analyses are also carried out by similar process. Then, homogenized constitutive equations are identified once more from numerical results.
3. In macroscale, finite element analysis considering damage propagation for LFT-D is performed using constitutive equations (mesoscale) and elastic moduli of fiber bundles.

Numerical methods (micro and mesoscales)

Homogenization method

- Elasto-viscoplasticity

Elasto-viscoplastic constitutive equation

$$\dot{\sigma}_{ij} = C_{ijkl}(\dot{\epsilon}_{kl} - \dot{\beta}_{kl}) \quad \dot{\epsilon}_{ij}^p = \dot{\beta}_{ij} = \frac{3}{2} \dot{\epsilon}_c \left[\frac{\sigma_{EQ}}{g(\bar{\epsilon}^p)} \right]^{\frac{1}{m}} \frac{\sigma_{ij}^D}{\sigma_{EQ}} \quad g(\bar{\epsilon}^p) = \sigma_c \left(\frac{\bar{\epsilon}^p}{\epsilon_c} \right)^n + C$$

Macroscopic constitutive equation

$$\dot{\sigma}_{ij}^H = \langle c_{ijpq}(\delta_{pk}\delta_{ql} + \chi_{p,q}^{kl}) \rangle \dot{\epsilon}_{kl}^H - \langle c_{ijkl}(\beta_{kl} - \varphi_{k,l}) \rangle$$

Microscopic stress evolution

$$\dot{\sigma}_{ij} = c_{ijpq}(\delta_{pk}\delta_{ql} + \chi_{p,q}^{kl}) \dot{\epsilon}_{kl}^H - c_{ijkl}(\beta_{kl} - \varphi_{k,l})$$

c_{ijkl} : Elastic stiffness

β_{ij} : Viscoplastic function

σ_{EQ} : Equivalent stress

σ_{ij}^D : Deviatoric stress

$\bar{\epsilon}^p$: Eq. viscoplastic strain

$\dot{\epsilon}_c$: Reference strain rate

m : Strain rate receptivity

σ_c : Reference stress

ϵ_c : Reference strain

n : Work-hardening index

C : Material parameter

Boundary value problems

$$\int_Y c_{ijpq} \chi_{p,q}^{kl} v_{i,j} dY = - \int_Y c_{ijkl} v_{i,j} dY$$

$$\int_Y c_{ijpq} \varphi_{p,q} v_{i,j} dY = \int_Y c_{ijkl} \beta_{kl} v_{i,j} dY$$

χ_i^{kl}, φ_i : Characteristic functions

Numerical methods (macroscale)

Finite element method

- Elasto-viscoplasticity
- Damage evolution

Elasto-viscoplastic constitutive equation

$$\dot{\sigma}_{ij} = C_{ijkl}(\dot{\epsilon}_{kl} - \beta_{kl}) \quad \dot{\epsilon}_{ij}^p = \beta_{ij} = \frac{3}{2} \dot{\epsilon}_c \left[\frac{\sigma_{EQ}}{g(\bar{\epsilon}^p)} \right]^{\frac{1}{m}} \frac{\sigma_{ij}^D}{\sigma_{EQ}} \quad g(\bar{\epsilon}^p) = \sigma_c \left(\frac{\bar{\epsilon}^p}{\epsilon_c} \right)^n + C$$

Grobal stiffness equation

$$\int_V \dot{u}_{i,j}^* c_{ijkl} \dot{u}_{k,l} dV = \int_S \dot{u}_i^* t_i dS + \int_V \dot{u}_{i,j}^* c_{ijkl} \beta_{kl} dV$$

c_{ijkl} : Elastic stiffness

β_{ij} : Viscoplastic function

σ_{EQ} : Equivalent stress

σ_{ij}^D : Deviatoric stress

$\bar{\epsilon}^p$: Eq. viscoplastic strain

σ_{ij}^{cr} : Critical stress

$\dot{\epsilon}_c$: Reference strain rate

m : Strain rate receptivity

σ_c : Reference stress

ϵ_c : Reference strain

n : Work-hardening index

C : Material parameter

Constitutive equation for damaged elements

$$\dot{\sigma}_{ij} = (1 - D)^2 C_{ijkl} \dot{\epsilon}_{kl} - \frac{\sigma_{ij}^{cr}}{\Delta t}$$

Grobal stiffness equation with damage evolution

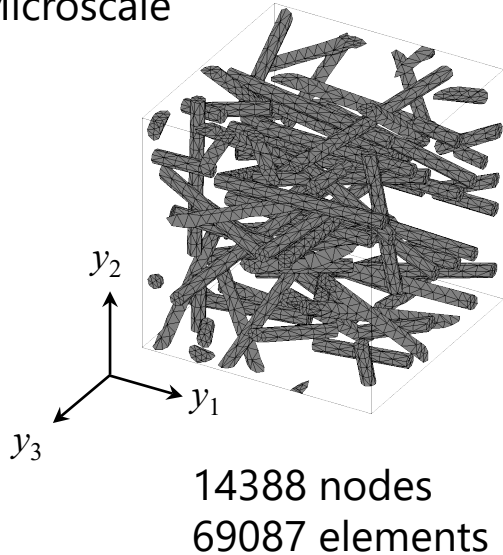
$$\int_V \dot{u}_{i,j}^* (1 - D)^2 c_{ijkl} \dot{u}_{k,l} dV = \int_S \dot{u}_i^* t_i dS + \int_V \dot{u}_{i,j}^* c_{ijkl} \beta_{kl} dV + \int_V \dot{u}_{i,j}^* \frac{\sigma_{ij}^{cr}}{\Delta t} dV$$

D : Damage variable

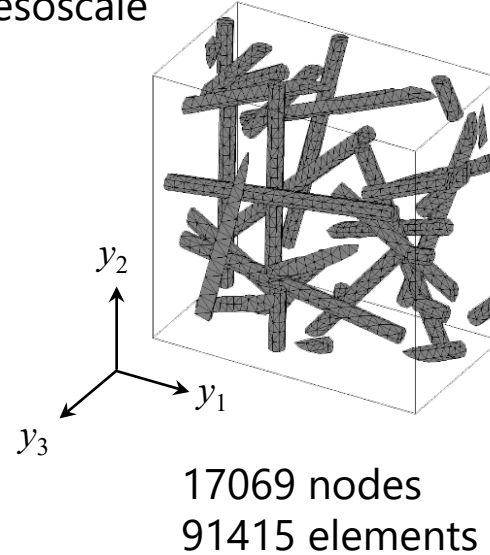
Numerical conditions (micro and mesoscales)

Finite element models

Microscale



Mesoscale



Loading conditions

Uniform constant tensile strain rates

$$\dot{\varepsilon}_{11}^H = 5.0 \times 10^{-2}, 5.0 \times 10^{-3}, 5.0 \times 10^{-4} \text{ s}^{-1}$$

Material parameters

Elastic moduli of carbon fiber (T700S)^[1]

$$E_L = 177.9 \text{ GPa} \quad E_T = 26.1 \text{ GPa} \quad G_{LT} = 23.9 \text{ GPa} \\ \nu_{LT} = 0.27 \quad \nu_{TT} = 0.77$$

Material parameters of resin (PA6)^[2]

$$E = 2.58 \text{ GPa} \quad \nu = 0.31 \\ \varepsilon_c = 0.02 \quad \dot{\varepsilon}_c = 0.015 \text{ s}^{-1} \\ \sigma_c = 19.3 \text{ MPa} \quad m = 0.037 \\ n = 0.14 \quad C = 55.7 \text{ MPa}$$

Elastic moduli of fiber bundles ($V_f = 65\%$)

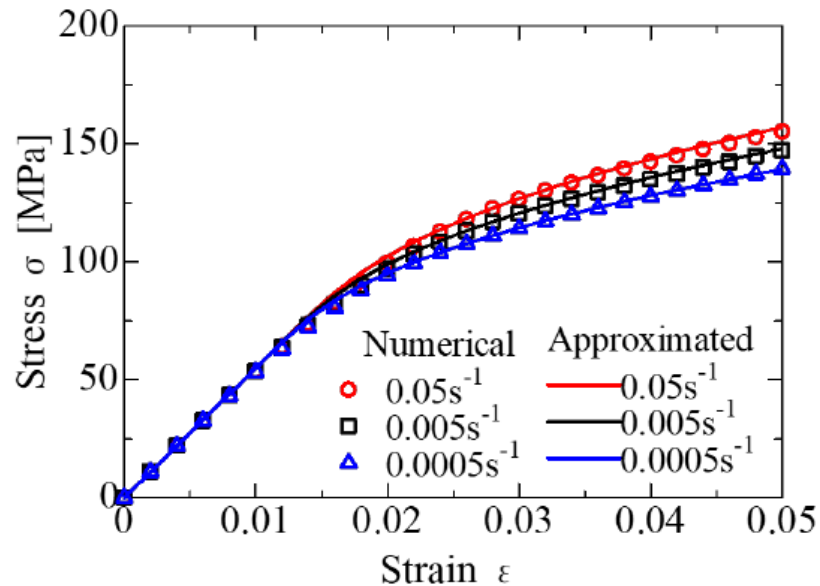
$$E_L = 116.4 \text{ GPa} \quad E_T = 8.40 \text{ GPa} \quad G_{LT} = 3.97 \text{ GPa} \\ \nu_{LT} = 0.28 \quad \nu_{TT} = 0.48$$

^[1]Kaku, et al., *Acta Mech.*, **214**, 111-121 (2010).

^[2]Goto, et al., *Trans. Jpn. Soc. Comput. Methods Eng.*, **16**, 115-120 (2016).

Numerical results (micro and mesoscales)

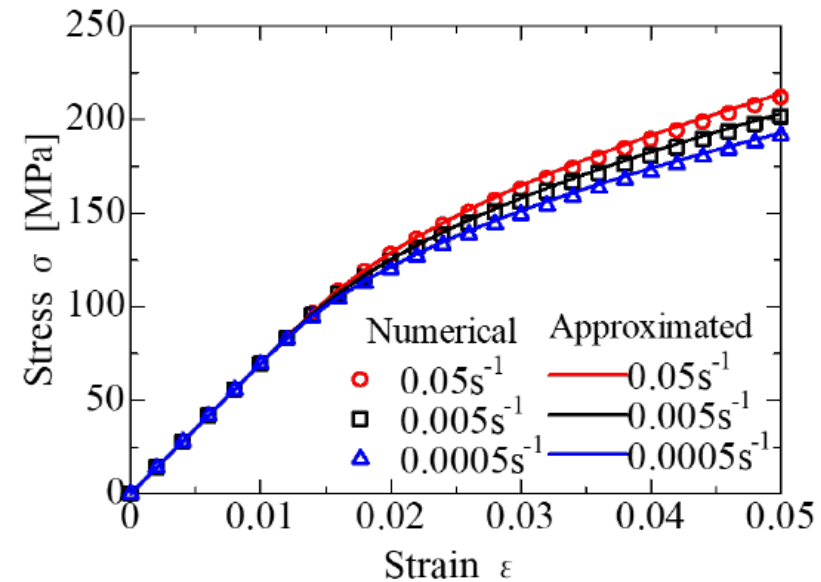
Microscale results



Identified material parameters from microscale

$E = 5.25 \text{ GPa}$	$\nu = 0.29$
$\epsilon_c = 0.02$	$\dot{\epsilon}_c = 0.005 \text{ s}^{-1}$
$\sigma_c = 89.2 \text{ MPa}$	$m = 0.031$
$n = 0.31$	$C = 57.8 \text{ MPa}$

Mesoscale results

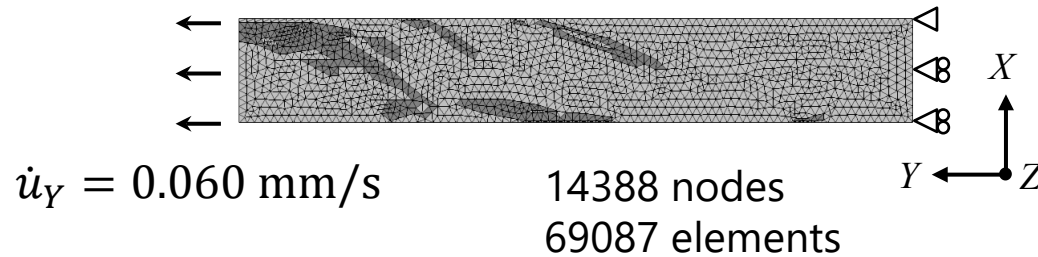


Identified material parameters from mesoscale

$E = 6.02 \text{ GPa}$	$\nu = 0.26$
$\epsilon_c = 0.02$	$\dot{\epsilon}_c = 0.005 \text{ s}^{-1}$
$\sigma_c = 110.8 \text{ MPa}$	$m = 0.037$
$n = 0.14$	$C = 68.8 \text{ MPa}$

Numerical and experimental conditions (macroscale)

Finite element model and boundary conditions



Material parameters

Elastic moduli of fiber bundles ($V_f = 65\%$)

$$E_L = 116.4 \text{ GPa} \quad E_T = 8.40 \text{ GPa} \quad G_{LT} = 3.97 \text{ GPa}$$

$$\nu_{LT} = 0.28 \quad \nu_{TT} = 0.48$$

Material parameters of matrix

$$E = 6.02 \text{ GPa} \quad \nu = 0.26$$

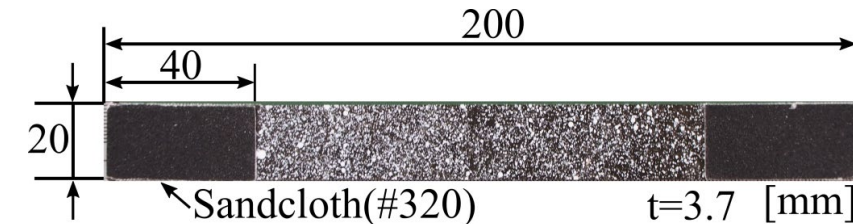
$$\varepsilon_c = 0.02 \quad \dot{\varepsilon}_c = 0.005 \text{ s}^{-1}$$

$$\sigma_c = 110.8 \text{ MPa} \quad m = 0.037$$

$$n = 0.14 \quad C = 68.8 \text{ MPa}$$

$$F^{cr} = 200 \text{ MPa}^{[3]}$$

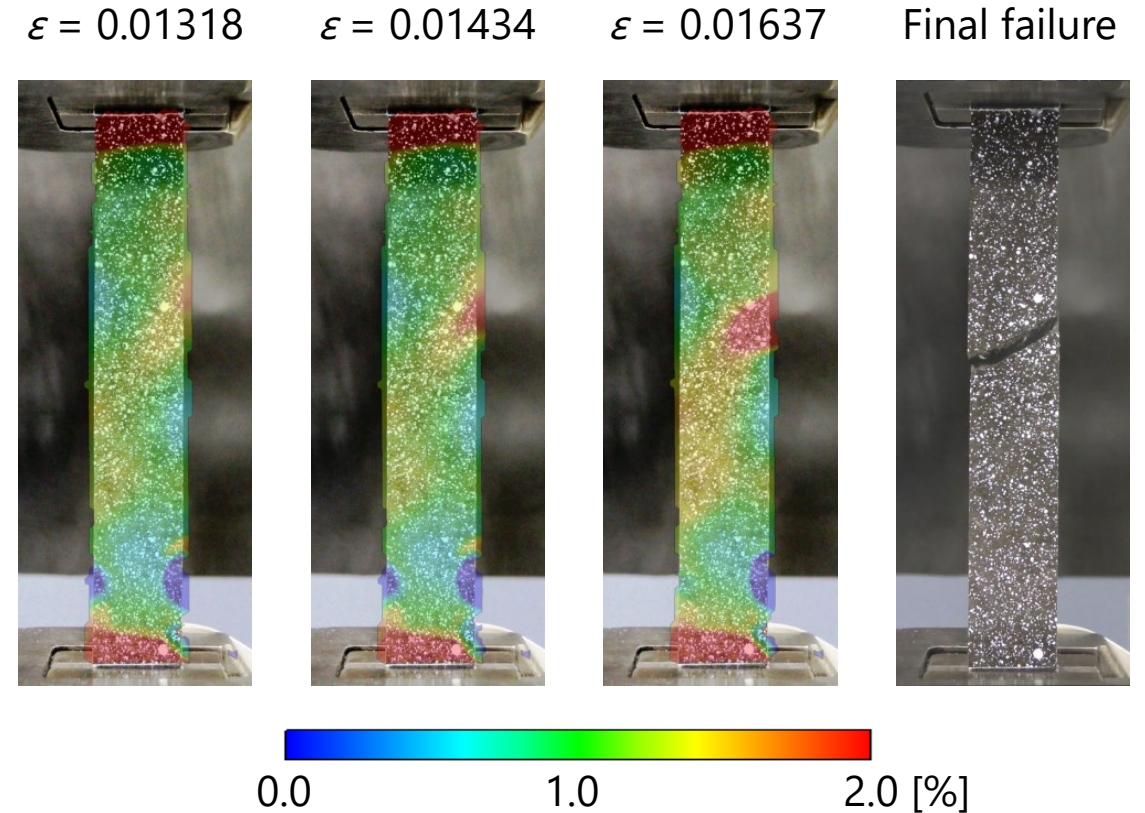
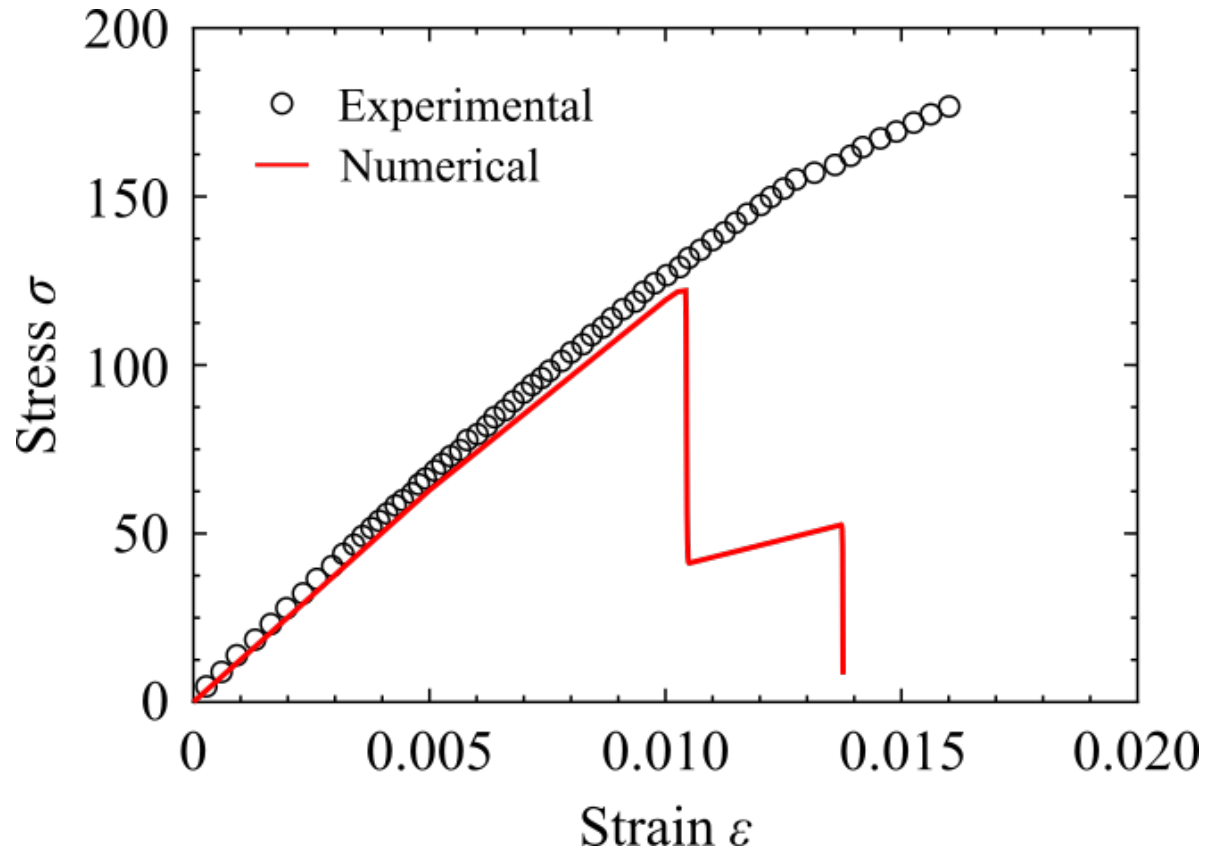
Tensile test specimen



- Tensile test of LFT-D was carried out by using same specimen prepared for X-ray CT observation.
- White random pattern was sprayed on evaluation area to analyze strain distribution by DIC method.
- Strain gage was glued on center of back side of specimen.
- Material test machine: AG-100kNXplus (Shimadzu)
- Digital video camera: HC-WX2M (Panasonic)
- Strain gage: KFGS-20-120-C1-11 (Kyowa)
- Crosshead rate: 10 mm/min

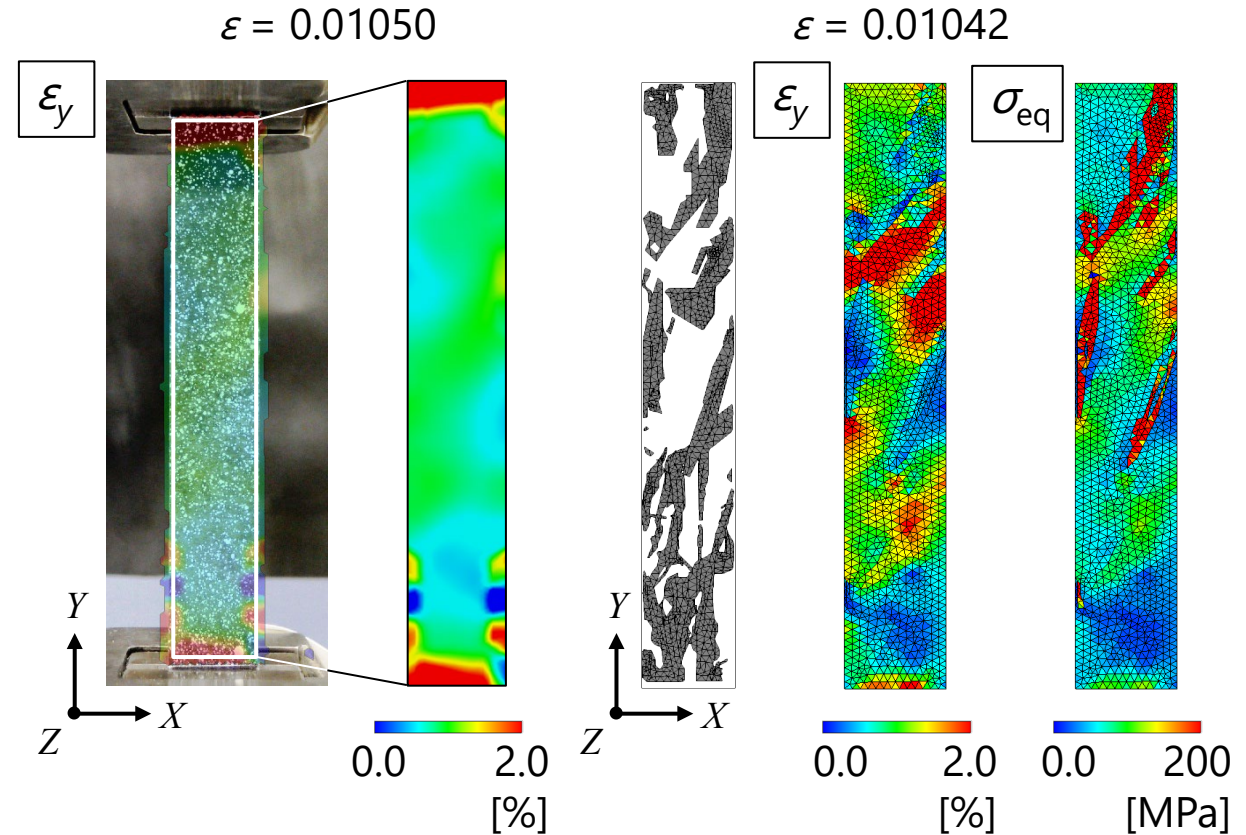
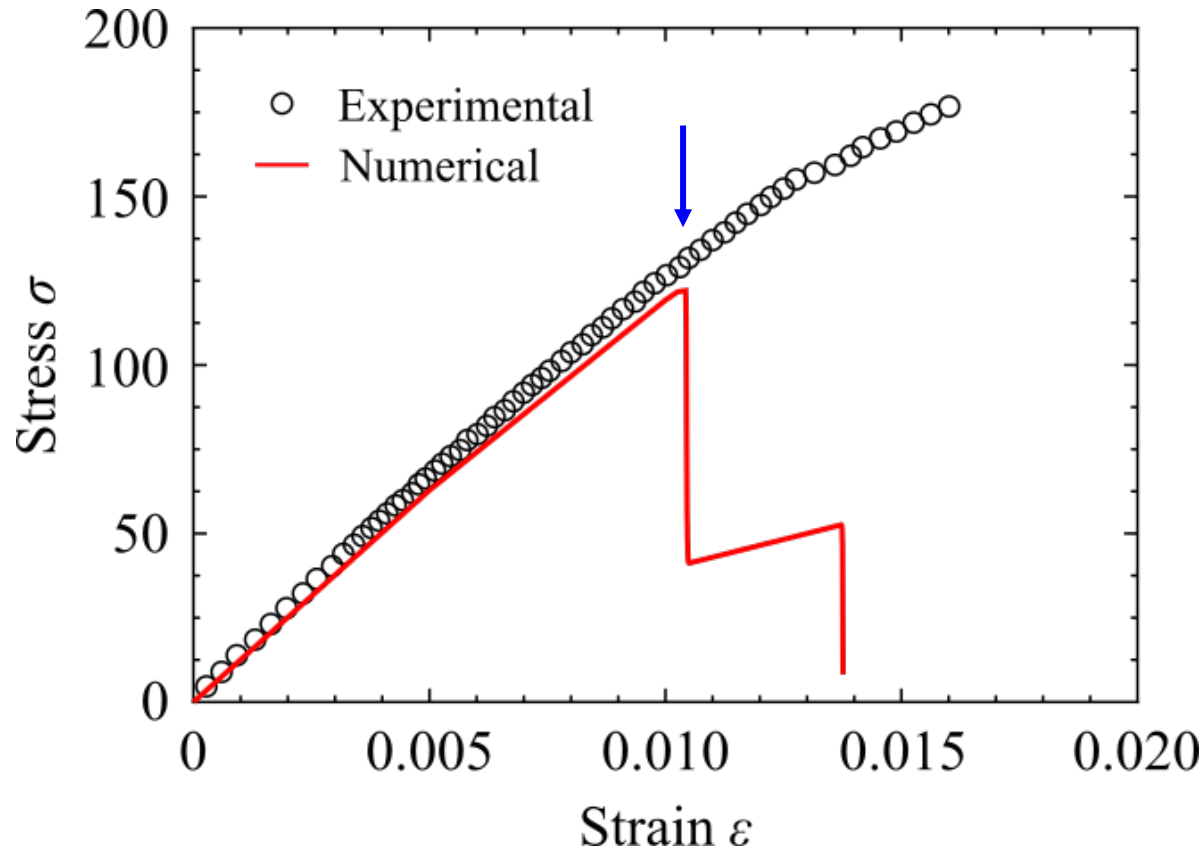
^[3]Hashimoto, et al., *Compos. Pt. A*, **43**, 1791-1799 (2012).

Stress-strain curve



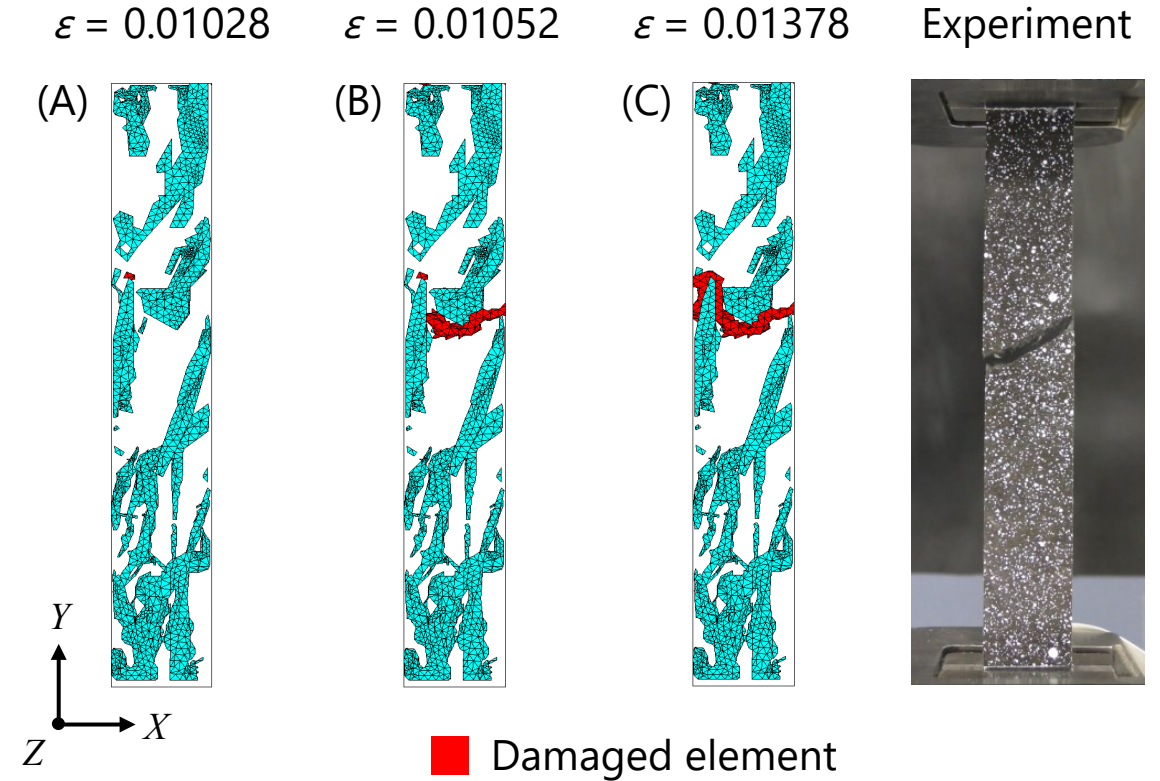
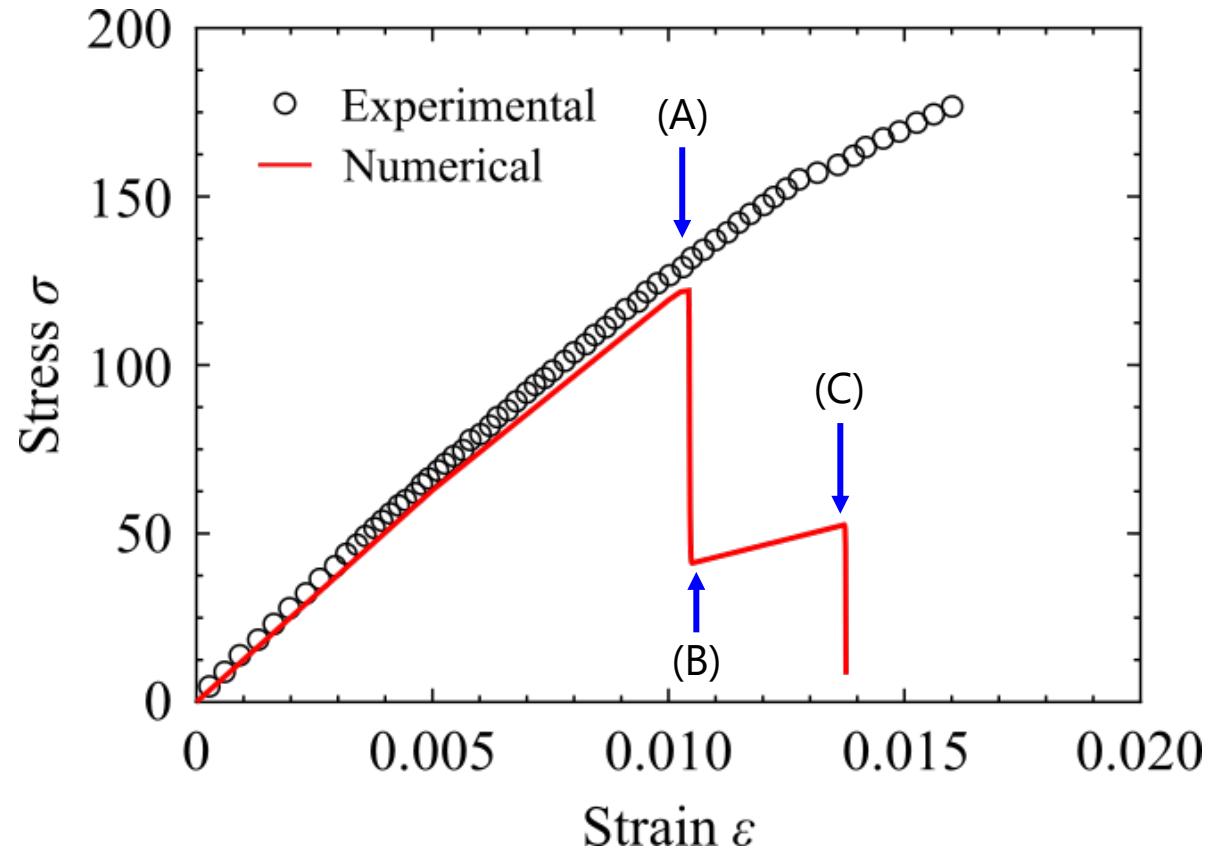
- In experiment, initial failure ($\varepsilon=0.014$) and final failure ($\varepsilon=0.016$) occurred.
- Drastic stress drop was found in early stage of numerical result ($\varepsilon=0.010$).

Stress/strain distribution



- Strain distributions showed similar tendency until stress drop occurred in numerical result.
- Strain and stress values tended to high in matrix region between fiber bundles.

Damage propagation



- Failure initiated from high strain area of specimen edge and propagated toward width direction.
- Similar trend can be seen in final failure aspects of numerical and experimental results.

Conclusions

In this study, elasto-viscoplastic property and damage propagation of LFT-D were evaluated based on multiscale numerical method consisting of three-scales.

- Internal structures of LFT-D were investigated and characteristic structures of LFT-D were observed in macro, meso, and microscales, respectively. Then, finite element models considering characteristic structures were prepared in each scale.
- Multiscale numerical method using homogenization method and finite element method was proposed. Elasto-viscoplasticity was considered in micro and mesoscales, and damage propagation of specimen was also taken into account in macroscale.
- Numerical results agreed well to experimental ones until initial failure occurred. Matrix region between fiber bundles exhibited high stress and strain values, which became origin of damage propagation of specimen.
- Stress-strain curve of numerical result dropped earlier because damage region propagated drastically in contrast to experimental result.